CORRELATION OF OBSERVED BUILDING PERFORMANCE WITH MEASURED GROUND MOTION

Stephanie A. King
Hart-Weidlinger, Weidlinger Associates, Inc.

Anne S. Kiremidjian
John Blume Earthquake Engineering Center, Stanford University

Pooya Sarabandi
John Blume Earthquake Engineering Center, Stanford University

Matthew Skokan
Saiful/Bouquet, Inc.

Abstract

This paper describes the progress to date on the CSMIP-funded project to develop correlations of observed building performance with measured ground motion. Model development is in progress to develop motion-damage relationships in the form of damage probability matrices and fragility curves for wood frame, steel moment frame, rehabilitated unreinforced masonry, concrete frame, and concrete shear wall buildings – building types for which there are enough samples in the database to warrant statistical analysis. Two sample motion-damage relationships for wood frame dwellings that have been developed with the project data are included with example applications. As this project is in progress, all data and models discussed in this paper are preliminary and likely subject to revision at a later date.

Introduction

Relationships between building performance and ground motion form the core of earthquake loss estimation methodologies, and are also used for structural analysis studies and in the design code formulation process. Currently-used motion-damage relationships are based primarily on models developed from expert opinion, such as ATC-13 (ATC, 1985), or models that combine analytical model results with expert opinion, such as HAZUS99 (FEMA, 1999). Attempts have been made to update the published motion-damage relationships with empirical data collected after damaging earthquakes (see Anagnos et al., 1995). Small improvements have been made to models for specific building types, but typically with the use of proprietary insurance loss data with inferred ground motion information.

Following the 1994 Northridge earthquake, an effort was made to systematically document the effects of earthquake shaking on structures adjacent to locations of strong ground motion recordings. The ATC-38 project (ATC, 2000) involved the inspection of more than 500 buildings located near (within 1000 feet of) 30 strong motion recording stations. The resulting database of building characteristic and performance documentation, photos, and strong motion recordings provides a wealth of information for developing new motion-damage relationships based on non-proprietary empirical data. A similar dataset was also developed following the recent Chi-Chi, Taiwan earthquake.

The purpose of the CSMIP-funded project discussed in this paper is to develop motion-damage relationships based on the correlation of observed building performance with measured ground motion parameters. The project tasks include: identifying and collecting appropriate datasets; analyzing, interpreting, and archiving data records; developing motion-damage relationships in the form of damage probability matrices and fragility curves; and illustrating the use of the final relationships. The remainder of this paper discusses these tasks in more detail and the status of the project, which at the current time is approximately 65% complete.

Dataset Collection

In order to develop meaningful and useful motion-damage relationship that correlate building performance to recorded ground motion data, the datasets have to satisfy certain criteria, including:

- Proximity to free-field ground motion recordings – building should be located close enough to strong motion recordings so that the shaking at the building site can be approximated as the shaking at the instrument site. Also, the building should not have any site-specific geologic conditions that might alter the ground shaking at the site.
- Non-proprietary – the datasets should contain information that is available to the general public so that other researchers may use the raw data, with their own proprietary data or with information collected after future earthquakes.
- Sufficient number of data points –statistical relationships will only be meaningful for those building classes with a large enough sample size.
- Consistent building survey information – building performance data should have been collected in a standard format with consistent inspector interpretation of qualitative and quantitative measures of damage.
- Unbiased with respect to building damage – datasets often include information only for damaged buildings. Statistical relationships will not be meaningful unless the datasets include information for both damaged and undamaged buildings.

The first task of the project was to identify and collect datasets that meet the above criteria, which were found to be very stringent. The following datasets were collected for use in the project:

- ATC-38 – Database on the Performance of Structures Near Strong-Motion Recordings: 1994 Northridge, California Earthquake (ATC, 2000)
- LADiv88 – Rutherford and Chekene Database on the Performance of Rehabilitated Unreinforced Masonry Buildings (Retrofitted According to Los Angeles Division 88 Standards) in the 1994 Northridge, California Earthquake (Lizundia and Holmes, 1997)

- SAC –Database on the Performance of Steel Moment Frame Buildings in the 1994 Northridge, California Earthquake (FEMA, 2000)
- Chi-Chi – Degenkolb Database on the Performance of Buildings Near Strong-Motion Recording Stations (Heintz and Poland, 2001)

Following the collection of the building performance datasets, the accompanying strong ground motion data were identified and collected. For the ATC-38 and Chi-Chi building datasets, the strong ground motion data are included as database tables linked via the attribute containing the building identification number. All buildings in these two datasets could be used in the analysis as they are all located very close (within 1000 feet) of the recording stations.

For the SAC and LADiv88 building datasets, only those buildings located near to free-field strong motion recording stations (and on similar site conditions) were extracted from the complete databases. This was done by mapping the building locations in a GIS and overlaying a map of the ground motion recording stations. Two classes of buildings were extracted from their respective datasets – those within 1000 feet of a recording station and those within 1 km of a recording station. The 1000 foot criterion was the approximate distance used in the ATC-38 and Chi-Chi datasets. The 1 km criterion was added so that at a later date (depending on project schedule) a sensitivity study of the distance criterion can be done.

The strong ground motion data for the stations identified within the vicinity of the SAC and LADiv88 buildings were obtained from several sources including:

- COSMOS – Consortium of Organizations for Strong-Motion Observation Systems Virtual Data Center, which contains links to strong ground motion from the California Division of Mines and Geology, the U.S. Geological Survey, the U.S. Bureau of Reclamation, and the U.S. Army Corps of Engineers (www.cosmos-eq.org)
- PEER – Pacific Earthquake Engineering Research Center Strong Motion Database (peer.berkeley.edu/smcat/)
- NGDC – National Geophysical Data Center Earthquake Strong Motion CD-ROM (www.ngdc.noaa.gov)

Table 1 shows a general distribution of the buildings extracted from the datasets for use in the project.

Ground Motion Analysis

Several ground motion parameters were identified as potential candidates for correlation with building performance data. The parameters include those deemed relevant to the intended use of the resulting motion-damage relationships, i.e., they are typically computed in loss estimation and design procedures.

The following parameters have been computed and archived for each strong motion data record:

- Time history data parameters (maximum of two horizontal components, average of two horizontal components, and vertical):
  - Peak ground acceleration (*PGA*)
  - Peak ground velocity (*PGV*)
  - Peak ground displacement (*PGD*)
  - ShakeMap Instrumental Intensity (I_{mm})
    From Wald et al. (1999), computed as a function of *PGA* in cm/sec^2 and *PGV* in cm/sec according to the following:
    $I_{mm} = 3.66 log(PGA) - 1.66$ for $I_{mm} < 7$ (1a)
    $I_{mm} = 3.47 log(PGV) + 2.35$ for $I_{mm} = 7$ (1b)
  - Duration (T_d)
    For the total record
    For the time period bracketed by 90% of the cumulative energy
    For the time period bracketed by a 0.05g cut-off acceleration level
  - Root mean square acceleration (a_{RMS})
    Computed from the acceleration time history *a(t)* for the three time durations (T_d) listed above as follows:
    $$a_{RMS} = \sqrt{\frac{1}{T_d} \int_0^{T_d} a(t)^2 \, dt} \qquad (2)$$
  - Arias Intensity (A_I)
    Computed from the acceleration time history *a(t)* for the three time durations (T_d) as follows:
    $$A_I = \int_0^{T_d} a(t)^2 \, dt \qquad (3)$$

- Response spectra data parameters (maximum of two horizontal components, average of two horizontal components, and vertical):
  - Acceleration spectrum intensity (*ASI*)
    Computed as the area under the acceleration response spectrum between 0.1 and 0.5 seconds (Von Thum et al., 1988)
  - Effective peak acceleration (*EPA*)
    Computed as the average of the acceleration response spectrum between 0.1 and 0.5 seconds, divided by 2.5 (ATC, 1978)
  - Effective peak velocity (*EPV*)
    Computed as the average of the velocity response spectrum between 0.8 and 1.2 seconds, divided by 2.5 (ATC, 1978)
  - Housner intensity (S_I)
    Computed as the area under the pseudo velocity response spectrum between 0.1 and 2.5 seconds (Housner, 1952)

- Spectral acceleration at several periods ($S_a(T)$)
- Spectral velocity at several periods ($S_v(T)$)
- Spectral displacement at several periods ($S_d(T)$)

- Others (not computed, but acquired through map overlays in GIS software):
  - Modified Mercalli Intensity (*MMI*)
  - Site class at the recording station site using the 1997 NEHRP Classification (FEMA, 1997)

Table 1. Approximate Distribution of Building Data for Use in Model Development

Building Type	Number of Building Records	
	Within 1000 ft of station	**1000 ft - 1 km from station**
Wood Frame	270	
Steel Frame	102	57
Concrete Frame	104	
Concrete Shear Wall	73	
Reinforced Masonry	89	
Unreinforced Masonry (URM)	18	
Rehabilitated URM	54	116
Precast	10	
TOTAL	720	173

Building Response Analysis

The building response datasets were initially analyzed for two purposes – to group the buildings into similar structural classes and to interpret the damage survey information. The grouping of buildings by structural class was done according to the FEMA 310 (FEMA, 1998) model building types shown in Table 2. This classification is similar to that used in the ATC-38 database; however, an important difference is the inclusion of model building type W1A to account for multi-story, multi-unit residences with tuck-under parking. For several of the classes shown in Table 2, the number of data points (see Table 1) is not sufficient to develop motion-damage relationships for those classes. As discussed in the next section, relationships are being developed for wood frame, steel moment frame, rehabilitated unreinforced masonry, concrete frame, and concrete shear wall buildings.

The building performance information required standardization in terms of damage to structural and nonstructural components. The following classifications are used for structural and nonstructural (if available) damage or performance:

- ATC-13 (ATC, 1985) – Damage states are as follows:
  - 1 = None = 0% loss

  - 2 = Slight = 0-1% loss
  - 3 = Light = 1-10% loss
  - 4 = Moderate = 10-30% loss
  - 5 = Heavy = 30-60% loss
  - 6 = Major = 60-100% loss
  - 7 = Destroyed = 100% loss
- HAZUS99 (FEMA, 1999) – Damage states are as follows:
  - None = 0% loss
  - Slight = 2% loss
  - Moderate = 10% loss
  - Extensive = 50% loss
  - Complete = 100% loss
- Vision 2000 (SEAOC, 1995) – Performance levels are as follows:
  - Fully Operational = 9-10 = Negligible damage
  - Operational = 7-8 = Light damage
  - Life Safe = 5-6 = Moderate damage
  - Near Collapse = 3-4 = Severe damage
  - Collapse = 1-2 = Complete damage
- FEMA 273/274 (FEMA, 1997) – Performance levels are as follows:
  - Operational = Very light damage
  - Immediate Occupancy = Light damage
  - Life Safety = Moderate damage
  - Collapse Prevention = Severe damage

In addition to the standardization of the structural classes and performance descriptions, the design code year and fundamental period were added to the database attributes associated with each building. The design code year is used to compute the design base shear (in terms of the seismic coefficient) and roof drift limit for each building. The fundamental period is used to compute the demand spectral values as described later in this section. For the general building types, the fundamental period is computed as a function of building height, *H*, as follows:

Wood frame building, based on Camelo et al. (2001):

$$T = 0.032H^{0.55} \tag{4}$$

Steel frame buildings, based on Chopra et al. (1998):

$$T = 0.035H^{0.80} \tag{5}$$

Reinforced concrete frame buildings, based on Chopra et al. (1998):

$$T = 0.018H^{0.90} \tag{6}$$

Rehabilitated unreinforced masonry buildings, based on UBC 1997 (ICBO, 1997):

$$T = 0.020H^{0.75} \tag{7}$$

Concrete shear wall buildings, based on UBC 1997 (ICBO, 1997):

$$T = 0.020H^{0.75} \tag{8}$$

Table 2. Model Building Types (from FEMA, 1998)

W1: Wood Light Frames	
W1	Single or multiple family dwellings
W1A	Multi-story, multi-unit residences with open front garages at the first story
W2: Wood Frames, Commercial and Industrial	
S1: Steel Moment Frames	
S1	Stiff diaphragms
S1A	Flexible diaphragms
S2: Steel Braced Frames	
S2	Stiff diaphragms
S2A	Flexible diaphragms
S3: Steel Light Frames	
S4: Steel Frame with Concrete Shear Walls	
S5: Steel Frame with Infill Masonry Shear Walls	
S5	Stiff diaphragms
S5A	Flexible diaphragms
C1: Concrete Moment Frames	
C2: Concrete Shear Wall Buildings	
C2	Stiff diaphragms
C2A	Flexible diaphragms
C3: Concrete Frame with Infill Masonry Shear Walls	
C3	Stiff diaphragms
C3A	Flexible diaphragms
PC1: Precast/Tiltup Concrete Shear Walls	
PC1	Stiff diaphragms
PC1A	Flexible diaphragms
PC2: Precast Concrete Frame	
PC2	Stiff diaphragms
PC2A	Flexible diaphragms
RM1: Reinforced Masonry Bearing Wall with Flexible Diaphragms	
RM2: Reinforced Masonry Bearing Wall with Stiff Diaphragms	
URM: Unreinforced Masonry Bearing Wall	
URM	Stiff diaphragms
URMA	Flexible diaphragms

The seismic demands on the building, in terms of displacement and base shear, have also being computed for each building in the dataset. This will allow for development and evaluation of relationships relating earthquake performance, not only to the recorded and computed ground motion parameters listed in the previous section, but also to seismic demand levels.

The estimate of building displacement demand during the recorded earthquake ground motion is computed as the spectral displacement demand normalized by the height of the building to obtain a *spectral drift ratio*. The spectral drift ratio, d_{S_d}, is calculated by the following:

$$d_{S_d} = S_d(T)/H \tag{9}$$

where $S_d(T)$ is the building spectral displacement demand obtained from the 5% damped response spectrum of the earthquake ground motion recorded at or near the building site, and H is the building height.

A minor inconsistency occurs when calculating the spectral drift ratio by Equation 9, due to the fact that the spectral displacement demand, based on an equivalent single degree-of-freedom system (SDOF), is normalized by the building height instead of an equivalent height of the SDOF system. In order to achieve consistency and also so that the demands can be compared to building code drift limits and FEMA 273 drift ratios related to building performance, the spectral drift ratio calculated in Equation 9 can be translated to an estimate of the building *roof drift ratio*. The roof drift ratio, d_R, is calculated by the following:

$$d_R = d_{S_d} C_0 = \frac{S_d(T) C_0}{H} \tag{10}$$

where C_0 is a modification factor that translates the spectral displacement demand, which represents the displacement of an equivalent SDOF system, to the roof displacement of the building. The value of C_0 depends on the dynamic characteristics of the building, and is based on the values provided by FEMA 273.

An effective measure of the ratio of building base shear demand to the building weight is the spectral acceleration, $S_a(T)$. The spectral acceleration is obtained from the 5% damped response spectrum of the earthquake ground motion recorded at or near the building site.

Preliminary Model Development

Motion-damage relationships are currently being developed in two forms – damage probability matrices (DPM) and fragility curves. DPMs show the conditional probability of being in a discrete damage state as a function of the input ground motion level, which can be a discrete value (e.g., *MMI*) or a range of values (e.g., *PGA*). The DPMs developed from the datasets are being fit to conditional probability distributions, typically Beta or lognormal distributions, although others will also be tested. Figure 1 illustrates with hypothetical data how the probability distribution corresponds to one column of the DPM. Fragility curves show the conditional probability of being equal to or exceeding a given damage state as a function of the ground motion parameter. Fragility curves are related to the DPMs and can be computed from them as shown, as they are essentially curves of the cumulative probability distribution for each damage state as a function of the ground motion level. Figure 1 shows how a fragility curve corresponds to a row (and the sum of the rows below) in the DPM.

DAMAGE PROBABILITY MATRIX					
	Probability (%) of being in a given damage state as a function of PGA for a given building type				
Damage State	PGA 0-0.2g	PGA 0.2-0.4g	PGA 0.4-0.6g	PGA 0.6-0.8g	PGA 0.8-1.0g
1, <2% loss	90	80	60	25	20
2, 2-10% loss	10	15	20	40	30
3, 10-30% loss	0	5	15	20	30
4, 30-60% loss	0	0	5	10	15
5, >60% loss	0	0	0	5	5

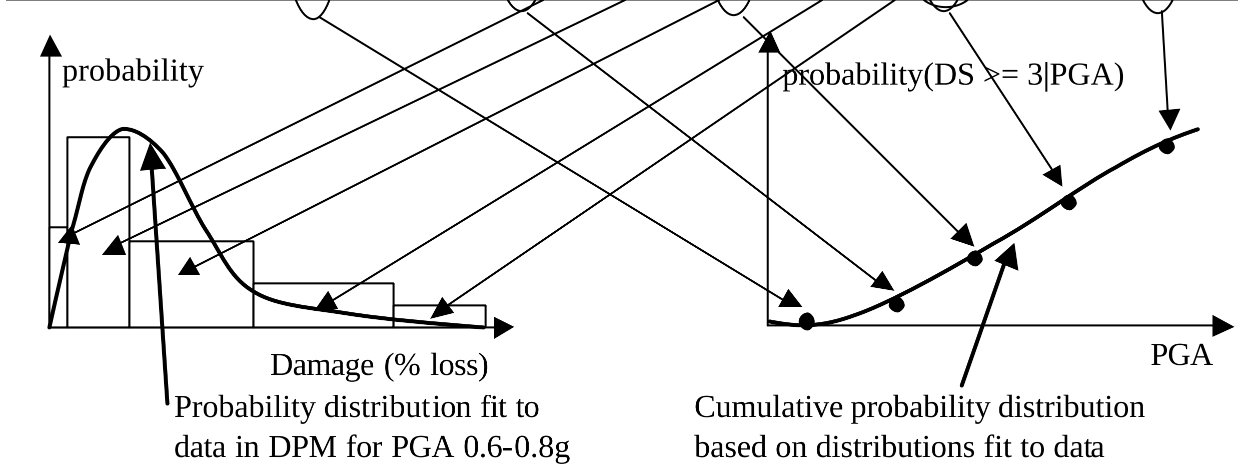

Figure 1. Illustration of DPM, probability distribution fit, and fragility curve.

In developing the motion-damage relationships, it is important to consider the relative uncertainty in the quality of the data, as the datasets have varying degrees of reliability and in some cases missing attributes had to be inferred from the reported data. This issue is being addressed when combining the data from the various sources by assigning weighting or quality factors to the data. Statistical analysis software is being utilized to aid in the development of the motion-damage relationships.

The final motion-damage relationships will be compared to those that are published in the literature (e.g., ATC-13 and HAZUS99). The comparison will include a discussion of how some of the motion-damage relationships developed in this project can be used to update current loss estimation models.

Example Models and Application

This section includes two motion-damage relationships that were developed from the data for wood frame dwellings (type W1). These relationships should be considered preliminary as the project is still in progress and the model development task has not yet been completed. The models presented here illustrate one form (DPM) of the relationships being developed, and their use for regional loss estimation and site-specific building evaluation.

The first model shows the relationship between building damage in terms of ATC-13 structural damage state and ShakeMap instrumental intensity, I_{mm}. The damage probability matrix shown in Table 3 gives, for each range in I_{mm}, the probability of being in one of seven damage states. The ATC-13 damage states each have an associated percent loss (in terms of percentage of replacement cost) as shown earlier in this paper. Using the mean of the range in percent loss for each damage state (termed the "central damage factor" in ATC-13) and the probabilities of being in each damage state, the expected loss can be computed for each range in I_{mm} as shown in Table 3.

Table 3. Preliminary Damage Probability Matrix for Wood Frame Dwellings (W1)

Damage State	Range in ShakeMap Intensity (I_{mm})					
	6-6.5	6.5-7.0	7-7.5	7.5-8	8-9	9-10
1	0.34	0.59	0.44	0.00	0.15	0.27
2	0.64	0.39	0.47	1.00	0.70	0.55
3	0.00	0.00	0.06	0.00	0.15	0.03
4	0.02	0.00	0.03	0.00	0.00	0.09
5	0.00	0.00	0.00	0.00	0.00	0.00
6	0.00	0.02	0.00	0.00	0.00	0.06
7	0.00	0.00	0.00	0.00	0.00	0.00
Expected Loss (%)	0.72	2.01	1.12	0.50	1.11	7.09

Figure 2 shows the application of the damage probability matrix given in Table 3. A ShakeMap showing Intensity (I_{mm}) computed for the 1994 Northridge earthquake in shown in Figure 2a. Figure 2b shows the distribution of expected loss to wood frame dwellings (W1) based on the data given in Table 3. This example illustrates the utility of a motion-damage relationship for making first order rapid estimate of earthquake damage immediately after an event.

The second model shows the relationship between building performance in terms of the FEMA 273 performance levels listed earlier in this paper and the roof drift ratio. The damage probability matrix shown in Table 4 gives, for each range in roof drift ratio, the probability of being in one of four performance states.

An example application of the damage probability matrix shown in Table 4 is for a site-specific performance-based building evaluation. For instance, using the FEMA 273 methodology, the site response acceleration spectra for the 10% in 50 year and 2% in 50 year hazard levels are as shown in Figure 3. Given a 2-story (H = 24 feet) wood frame dwelling with a fundamental period of 0.184 sec (computed according to Equation 4), the spectral acceleration values are obtained from Figure 3 and converted to spectral displacement values. Roof drift ratios are computed according to Equation 10, using $C_0 = 1.2$. Using the relationship shown in Table 4, the probability of the various performance levels is computed for the two hazard levels, thus giving a first order approximation of the likelihood of meeting the performance objectives for the building (e.g., immediate occupancy for both the 2% in 50 year and 10% in 50 year ground shaking hazard levels). Table 5 shows the results of this exercise.

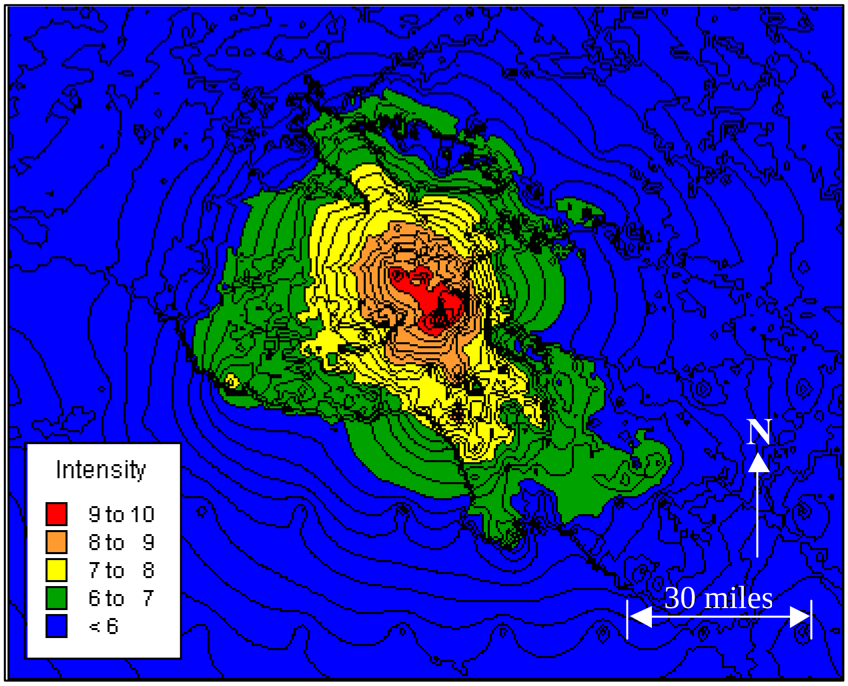

Figure 2a. ShakeMap showing Intensity distribution for the 1994 Northridge earthquake.

The model development phase of the project is in progress. The two models included in this section represent a very small sample of the motion-damage relationships that are being developed as part of this project. As these models are preliminary and subject to revision, comments will not be made in this paper with respect to the appropriateness of the models for the applications illustrated here, the uncertainty, the comparison with other published models, and other discussion points that will be included in the final project report.

Summary

This paper describes the progress to date on the CSMIP-funded project to develop correlations of observed building performance with measured ground motion. The necessary datasets have been collected, screened, and archived. Ground motion and building response parameters have been computed. Model development is in progress to develop motion-damage relationships in the form of damage probability matrices and fragility curves for wood frame, steel moment frame, rehabilitated unreinforced masonry, concrete frame, and concrete shear wall buildings – building types for which there are enough samples in the database to warrant statistical analysis.

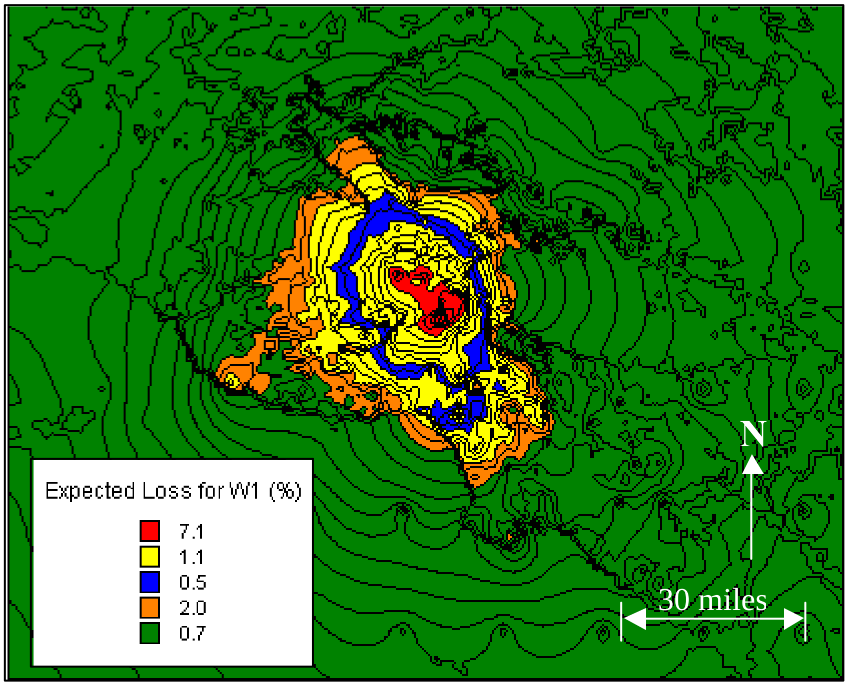

Figure 2b. **ShakeMap showing distribution of expected loss for wood frame dwellings in the 1994 Northridge earthquake based on data in Table 3.**

Table 4. **Preliminary Damage Probability Matrix for Wood Frame Dwellings (W1)**

Performance Level	Range in *Roof Drift Ratio* (%)				
	< 0.045	0.045-0.06	0.06-0.075	0.075-0.12	> 0.12
Operational	0.34	0.59	0.44	0.00	0.15
Immediate Occupancy	0.64	0.39	0.47	1.00	0.70
Life Safety	0.00	0.00	0.06	0.00	0.15
Collapse Prevention	0.02	0.00	0.03	0.00	0.00

Two sample motion-damage relationships for wood frame dwellings that have been developed with the project data are included. The use of these relationships is illustrated by application to regional rapid loss estimation and site-specific building evaluation. As this project is in progress and not scheduled to be completed for another six months, all data and models discussed in this paper are preliminary and likely subject to revision at a later date.

Acknowledgements

The authors would like to sincerely thank the following individuals who provided valuable data for use in the project: David Bonowitz, Bret Lizundia, and Chris Poland.

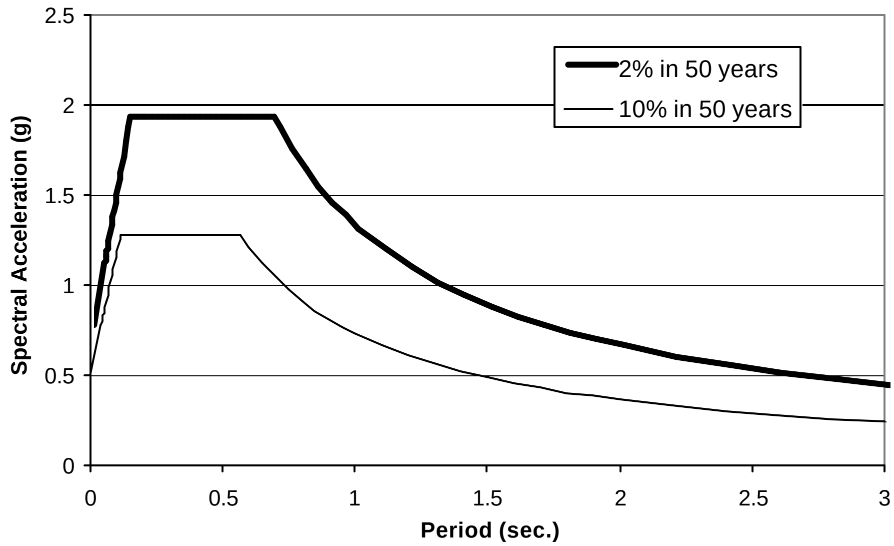

Figure 3. Example site-specific acceleration response spectra.

Table 5. Results of Example Site-Specific Building Evaluation

	2% in 50 year Hazard	**10% in 50 year Hazard**
Spectral Acceleration (g)	1.92	1.28
Spectral Displacement (in.)	0.623	0.416
Roof Drift Ratio (%)	0.26	0.17
P(Operational Performance)	0.15	0.15
P(Immediate Occupancy)	0.70	0.70
P(Life Safety)	0.15	0.15
P(Collapse Prevention)	0.00	0.00

References

Anagnos, T., Rojahn, C., and Kiremidjian, A., 1995, *NCEER-ATC Joint Study on Fragility of Buildings,* Technical Report NCEER-95-0003, National Center for Earthquake Engineering Research, State University of New York at Buffalo.

ATC, 2000, *Database on the Performance of Structures Near Strong-Motion Recordings: 1994 Northridge, California, Earthquake,* ATC-38 Report, Applied Technology Council, Redwood City, CA.

ATC, 1985, *Earthquake Damage Evaluation Data for California*, ATC-13 Report, Applied Technology Council, Redwood City, CA.

ATC, 1978, *Tentative Provisions for the Development of Seismic Regulations for Buildings*, ATC-3-06 Report, Applied Technology Council, Redwood City, CA.

Camelo, V.S., Beck, J.L., and Hall, J.F., 2001, *Dynamic Characteristics of Woodframe Buildings*, CUREE-Caltech Woodframe Project Report, Consortium of Universities for Research in Earthquake Engineering, Richmond, CA.

Chopra, A.K., Goel, R.K., and De la Llera, J.C., 1998, "Seismic Code Improvements Based on Recorded Motions of Buildings During Earthquakes," in *Proceedings of SMIP 98 Seminar on Utilization of Strong-Motion Data*, California Strong Motion Instrumentation Program, Division of Mines and Geology, Sacramento, CA.

FEMA, 2000, *Recommended Seismic Evaluation and Upgrade Criteria for Existing Welded Steel Moment-Frame Buildings*, Report FEMA-351, Prepared by the SAC Joint Venture for the Federal Emergency Management Agency, Washington, DC.2000.

FEMA, 1999, *HAZUS Earthquake Loss Estimation Methodology*, Technical Manual, Prepared by the National Institute of Building Sciences for the Federal Emergency Management Agency, Washington, DC.

FEMA, 1998, *Handbook for the Seismic Evaluation of Buildings – A Prestandard*, Report FEMA 310, Prepared by the American Society of Civil Engineers for the Federal Emergency Management Agency, Washington, DC.

FEMA, 1997, *NEHRP Guidelines for the Seismic Rehabilitation of Buildings*, Federal Emergency Management Agency, Report FEMA-273, Washington, DC.

Heintz, J.A. and Poland, C.D., 2001, "Correlating Measured Ground Motion with Observed Damage," *Earthquake Spectra*, Supplement A to Volume 17, pp. 110-130.

Housner, G.W., 1959, "Behavior of Structures During Earthquakes," *Journal of the Engineering Mechanics Division*, American Society of Civil Engineers, Vol. 85, No. EM14, pp 109-129.

ICBO, 1997, *Uniform Building Code*, International Conference of Building Officials, Whittier, CA.

Lizundia, B. and Holmes, W.T., 1997, "The performance of rehabilitated URM buildings in the Northridge earthquake," *Proceedings of the NEHRP Conference and Workshop on Research on the Northridge, California Earthquake of January 17, 1994*, California Universities for Research in Earthquake Engineering (CUREe), Richmond, California, Vol. III-A, 1998, pages III-116 -- III-123.

SEAOC, 1995, *Performance based seismic engineering of buildings (Vision 2000)*, Structural Engineers Association of California, Sacramento, CA.

Wald, D.J., Quitoriano, V., Heaton, T.H., and Kanamori, H., 1999, "Relationships between Peak Ground Acceleration, Peak Ground Velocity, and Modified Mercalli Intensity in California," *Earthquake Spectra*, Vol. 15, No. 3, pp 557-564.